Complex networks in confined comminution

David M. Walker and Antoinette Tordesillas*
Department of Mathematics and Statistics, University of Melbourne, Parkville, VIC 3052, Australia

Itai Einav
School of Civil Engineering, The University of Sydney, Sydney, NSW 2006, Australia

Michael Small
Department of Electronic and Information Engineering, Hong Kong Polytechnic University, Hung Hom, Kowloon, Hong Kong

(Received 2 November 2010; revised manuscript received 14 June 2011; published 8 August 2011)

The physical process of confined comminution is investigated within the framework of complex networks. We first characterize the topology of the unweighted contact networks as generated by the confined comminution process. We find this process gives rise to an ultimate contact network which exhibits a scale-free degree distribution and small world properties. In particular, if viewed in the context of networks through which information travels along shortest paths, we find that the global average of the node vulnerability decreases as the comminution process continues, with individual node vulnerability correlating with grain size. A possible application to the design of synthetic networks (e.g., sensor networks) is highlighted. Next we turn our attention to the physics of the granular comminution process and examine force transmission with respect to the weighted contact networks, where each link is weighted by the inverse magnitude of the normal force acting at the associated contact. We find that the strong forces (i.e., force chains) are transmitted along pathways in the network which are mainly following shortest-path routing protocols, as typically found, for example, in communication systems. Motivated by our earlier studies of the building blocks for self-organization in dense granular systems, we also explore the properties of the minimal contact cycles. The distribution of the contact strain energy intensity of 4-cycle motifs in the ultimate state of the confined comminution process is shown to be consistent with a scale-free distribution with infinite variance, thereby suggesting that 4-cycle arrangements of grains are capable of storing vast amounts of energy in their contacts without breaking.

DOI: 10.1103/PhysRevE.84.021301 PACS number(s): 81.05.Rm

I. INTRODUCTION

Comminution is the process of grain-size reduction through crushing, cutting, breaking and grinding. It is pivotal to many operations in a wide range of industries, including mineral processing, agriculture, pharmaceuticals, and in geoscience. To investigate comminution problems, we have previously developed a two-dimensional crushable discrete element (DEM) model [1,2] (see Fig. 1). Based on those model simulations, it was found that such systems develop a power-law grain size distribution (see Fig. 2, inset), in agreement with previous DEM results [3], cellular automata models [3,4], experiments [5], and geological evidence [4,6]. The ability of our numerical model to capture the realism of this process was further reaffirmed by detecting a well-known observation in soil mechanics, which was attributed to grain crushing [7]: the quite sudden transition of the associated porosity-pressure curve toward a logarithmic relation (see Fig. 2). Our work demonstrated that the notion of an ultimate power-law grain size distribution is intimately linked to a clear lognormal contact force distribution [2], while the network of the force chains congests as the system evolves toward a self-similar fractal pattern [1]. Furthermore, it was revealed that this process is characterized by transient chaos toward a multiple fixed-point attractor at the congestion point [2]. Here, we examine the evolution of a confined comminution system within the framework of complex networks to quantitatively characterize emergent properties inherent in the rheological response of the material.

Although the network properties of granular systems (e.g., the network of contacts and contact forces) have received considerable attention in the extant literature, the majority of these have been confined to static packings and noncomminuting systems and, more importantly, do not formally exploit the techniques of complex networks (e.g., [8–11]). This is somewhat surprising given the demonstrated utility and versatility of complex networks in extracting new insights into self-organization and emergent behavior in an increasingly broad range of real-world complex networks [12–18]. By drawing connections to other areas of complex systems (e.g., soft matter physics), Smart and Ottino [19] were among the first to bridge this glaring gap. In Ref. [19] they present an illuminating introduction to and a compelling case for the analysis of granular media problems using a networks approach. Subsequent nascent attempts at a formal application of complex network techniques to the evolution of fabric (i.e., contacts) and contact force anisotropies in a deforming granular medium have uncovered new clues to the nature of granular deformation and the intricate coupling between kinematical rearrangements and force transmission [20–22]. Indeed these studies have been pivotal in the latest discoveries from the studies of Tordesillas *et al.* [23,24] and of Arevalo *et al.* [25], which have elucidated the role of mesoscopic building blocks for self-organization through network motifs. Motifs are recurring patterns in a network which occur more frequently

*atordesi@ms.unimelb.edu.au

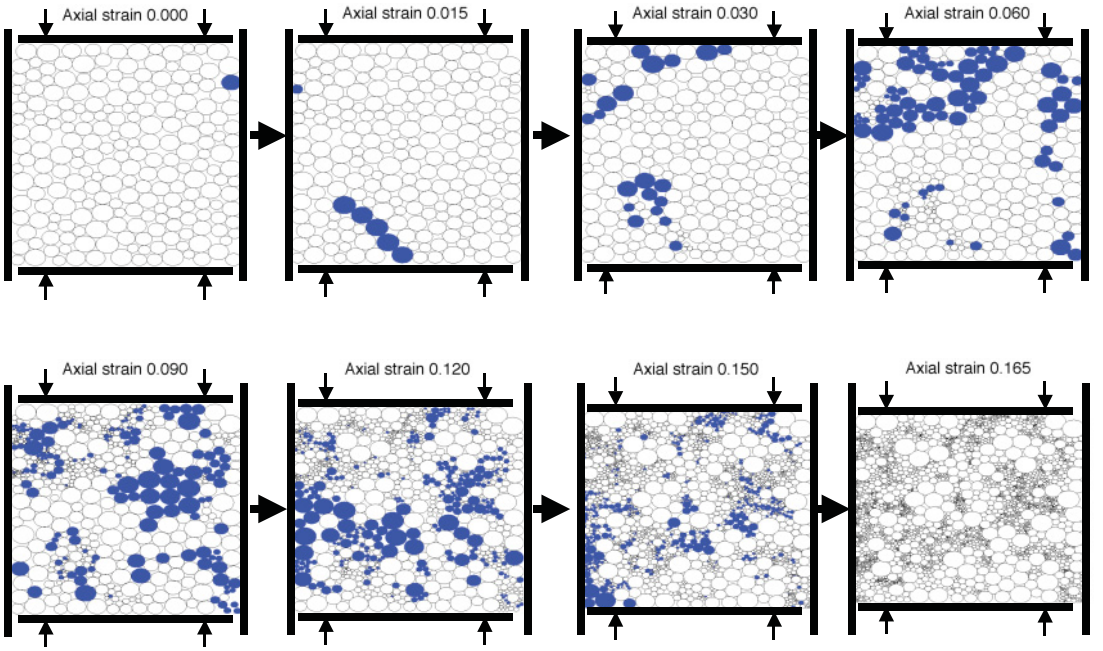

FIG. 1. (Color online) Consecutive axial strain stages of the DEM simulation with illustrative uniaxial boundary conditions. The axial load is increased gradually by bringing the upper and lower walls closer at a relative inwards velocity that grows slowly to 3 mm/sec. Filled circles show which particles fracture between observations. Two elements determine if a given particle fractures: (i) the local topology of the contact forces and stresses and (ii) internal defects modeled by strength thresholds drawn from a Weibull distribution [1].

than in random networks, and thus hint at possible functional mechanisms underpinning system evolution. The functional significance of such patterns in granular systems under load (e.g., how such motifs promote the transmission of force and enhance the global stability of the deforming granular body) have been explored in experiment and in discrete element (DEM) simulations [23,26,27]. The building blocks comprise quasilinear and cyclic structures: the so-called force chains and the minimal contact cycles. Columnar force chains are the primary structures which bear the majority of the load and serve as the central repositories for stored strain energy. Conjoined with these strong axially-loaded force chain columns are the secondary structures of minimal contact cycles: these involve comparatively weakly loaded contacts that provide confining lateral support to force chains [23]. Understanding the nature of cooperative behavior among building blocks of linear force chains and their supporting minimal cycles is key to the rheology of materials. In the absence of grain breakage, particle kinematics (i.e., frictional rearrangements) drive the evolution of force chains and contact cycles. In confined comminution, however, we have the added effect of grain breakage that enriches the self-organization process as the grain population grows and the particle size distribution widens. The study we report in the next sections provides a complex networks analysis of granular rheology in the presence of grain breakage.

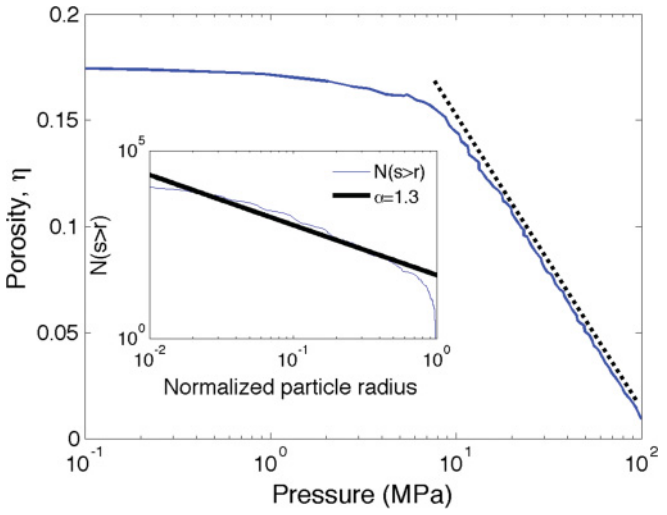

FIG. 2. (Color online) Porosity-pressure curve and (inset) grain size distribution at the ultimate strain.

The process of self-organization in confined comminution systems generates a richly evolving complex network with a fascinating array of features that are quite revealing of the underpinning dynamics throughout loading. For example, the grains in Fig. 1 shows the response to crushing with increasing axial strain in our confined uniaxial compression system with the grains that break between the intervals distinguished here by their solid dark color. Although this may already hint at some interesting phenomena (e.g., the tendency of the system to develop local "avalanches" of grains crushing), this is only a qualitative deduction. Distinguished from this particular observation and, in fact, most previous work in the area, this paper proceeds with a quantitative investigation within the framework of complex networks. At each strain state of the loading history, the complex network can be constructed by assigning a node to each particle and a connecting link between nodes if their corresponding particles are in physical contact. This results in an unweighted, undirected graph. Further information can be included such as the contact force or strain

energy at contacts to obtain a weighted complex network. In this study, we track the evolving properties of the networks and motif structures within the networks as comminution proceeds.

Our objectives are threefold. First, we aim to quantitatively characterize the topology of the contact networks, as generated by the comminution process. We are particularly interested in the evolution to the ultimate state and the properties of the limiting network to which the process of comminution evolves. Second, we hope to gain new insights into the rules (if any) that drive self-organization of the strong versus weak forces transmitted at the contacts and how these relate to the underlying topology of the global contact network. Can we extract trends that suggest the possibility of certain network properties being optimized in the individual stages of loading? To what extent does contact topology govern the self-organization of the load-bearing structures of force chains in the system? Of interest also are the secondary building blocks of minimal cycles which support the primary linear building blocks of force chains. Accordingly, our third objective is to explore this connection from the standpoint of strain energy intensity in the dominant members of the minimal contact cycle basis for this confined comminution system (i.e., 3-cycles and 4-cycles).

This paper is arranged as follows: We first describe the discrete element model of comminution under uniaxial compression. Next we quantitatively characterize the network at the ultimate state and explore the extent to which it exhibits scale-free and small world characteristics. We then discuss the relationship between shortest-path network measures and force transmission before discussing the energy content of cycle subgraph motifs within the ultimate state network.

II. DISCRETE ELEMENT MODEL

We use the discrete element method to model the process of grain rearrangements and crushing under confined uniaxial compression. This model has been described in detail elsewhere [1]. For completeness, we briefly summarize the salient features of this model here. The model of the process of confined comminution, exemplified in Fig. 1, bears two parts. The first concerns the grain fracture criterion; the second deals with the resulting post-fracture configuration. We employ the grain fracture criterion of [28] as follows: We first calculate the major and minor principal representative forces acting on a given particle using

$$\lambda_{\pm} = \frac{s_{11}+s_{22}}{2} \pm \sqrt{\left(\frac{s_{11}-s_{22}}{2}\right)^2 + s_{12}s_{21}}, \qquad (1)$$

where $s_{ij} = \sum_{c=1}^{N_c} n_i^{(c)} F_j^{(c)}$ denotes an effective force moment tensor per particle, N_c is the grain's coordination number, the superscript c stands for the cth contact. the subscripts i and j represent the ith and jth components of the unit normal vector $n_i^{(c)}$, and $F_j^{(c)}$ is a contact force vector [29]. The representative measures of the shear and normal forces per particle are computed via $\Theta = (\lambda_+ - \lambda_-)/2$ and $\Gamma = (\lambda_+ + \lambda_-)/2$, respectively. A particle of diameter x crushes if the modified "Brazilian" criterion of $2\Theta - \Gamma \geqslant x\sigma_f$ is met; here σ_f denotes the particle's strength according to $\sigma_f \equiv \sigma_f(P) = \sigma_{fM}\ln(1/P)^{1/w}(x/x_M)^{-2/w}$. Following Jaeger [30], σ_{fM} is the critical tensile stress for the failure of the biggest particle with a size x_M; the factor $\ln(1/P)^{1/w}$ is used to capture Weibull's statistics of strengths [31], while $P \in [0,1]$ is a uniformly distributed random variable.

The second part of the model, which concerns the post-fracture configuration when a grain exceeds the failure criterion, follows the well-established strategy of replacing the pre-crushed particle by post-fracture fragments [32]. Here, the pre-crushed "parent" particle is replaced by a set of three identical smaller fragments, inscribed within the circumference of the parent particle. This is achieved without introducing overlaps and without limiting the number of fragment generations or their size. Mass is conserved by a rapid linear expansion of the fragments, while carefully avoiding artificial effects in a two-phase process [1]. During the first phase a grain fractures into three fragments, which are seeded and randomly rotated in the site of the original grain without conserving the mass. A second phase of rapid linear expansion is introduced to recover any lost original mass. This mass conservation strategy is validated by the presence of two distinct dynamic time scales during crushing: (i) a local timescale where the arrangement of grain fragments are prescribed and (ii) a global timescale determined by the uniaxial compression boundary conditions. The expansion process to preserve mass was carefully chosen to be faster than the local timescale and here a time less than 0.002% of the total simulation time was deemed adequate for all practical purposes. This process of growing to conserve mass is similar to the way shapes in (Apollonian) packings are seeded and grown until contact is achieved [33–35]. Of course, in these applications no deformation, breakage, or force information is in play, although a shape rotation can be allowed to improve aspects of the resultant packing [35].

More than 200 particles with normal and shear stiffness of 10^3 MPa (MN/m per 1 m thickness unit) are introduced into a rectangular loading chamber, with normal and shear stiffness of 10^5 MPa. The system consolidates to the jamming transition between the fluid and solid phases [36]. Motivated by experiments on brittle sand, particle density is set to 2000 kg/m^3, $w = 4$, $\sigma_{fM} = 18$ MPa, and the largest grain is taken to be $x_M = 6$ mm. An initial uniform distribution of grain sizes by number, where the smallest initial grain size x_m, is set to give $x_M/x_m = 2$. The intergranular friction coefficient μ is chosen to be 0.6 while keeping the side walls fixed. The axial load is increased gradually by bringing the upper and lower walls closer at a relative inwards velocity that grows slowly to 3 mm/sec. The simulation is continued until an asymptotic limit is observed in each of the evolving grain size distribution and contact force distribution—shown in [2] to be well described by a lognormal distribution. The ultimate power law grain size distribution with a fractal random self-similar pattern is in agreement with previous experimental, numerical, and theoretical observations [3,4,6,37,38]. Readers are referred to Refs. [1,2] for complete details of the simulation for certain fractal properties of the ultimate state established to date.

III. EVOLUTION TO A SCALE-FREE, SMALL WORLD NETWORK

Research in complex networks has been driven by efforts to classify networks found in the real world by their degree

distribution with power law distributions being of particular interest. The degree of a contact network node is synonymous with a particles coordination number. The power law exponent has important implications for the system the network represents. For example, it can be a factor as to whether a disease epidemic continues to spread or eventually dies out in a population [39]. The process of comminution represented here and elsewhere has been shown to evolve to an ultimate grain size distribution consistent with a power law, as well as to exhibit self-similar properties. Indeed, the ultimate grain size distribution matches statistics of certain generations of an Apollonian gasket [2,40]. Apollonian gaskets induce Apollonian complex networks, which have power law degree distributions, and also exhibit small world network properties. Given the parallels between the grain size distribution of the crushable DEM model and the Apollonian gasket, it might be expected then that the ultimate contact network induced by comminution should result in a scale-free network with small world properties. It is worth mentioning, however, that typically geographical or spatial scale-free networks are not necessarily small world (e.g., a network constructed from avian flu outbreak data [41]; see also [42]).

Scale-free networks contain nodes with very high number of links or edges (so-called hubs) and the degree distribution follows a power law; that is, most nodes have only a small number of links while a small fraction of nodes have a very high number of links. We have used the maximum likelihood power law fitting method described in [43] to fit a discrete degree distribution: $p(x) \propto x^{-\alpha}$ for $x \geqslant x_{\min}$ where x denotes the degree of a network node. The significance of the fit is determined by bootstrap resampling and the Kolmogorov-Smirnov (KS) statistic. The ultimate state of the crushable DEM yields a complex network with a power law parameter of $\alpha = 4.211$ and $x_{\min} = 5$. The fit passed the KS test [43], thus giving good supporting evidence that the degree distribution of the contact network of the ultimate state of the crushable DEM is scale free. (See Fig. 3(a) showing the fit and the empirical cumulative distribution function.) This finding is consistent with the power law grain size distribution: here the hubs are the large particles, which are surrounded by a high number of connections or contacts with the small particles that form the majority of the assembly.

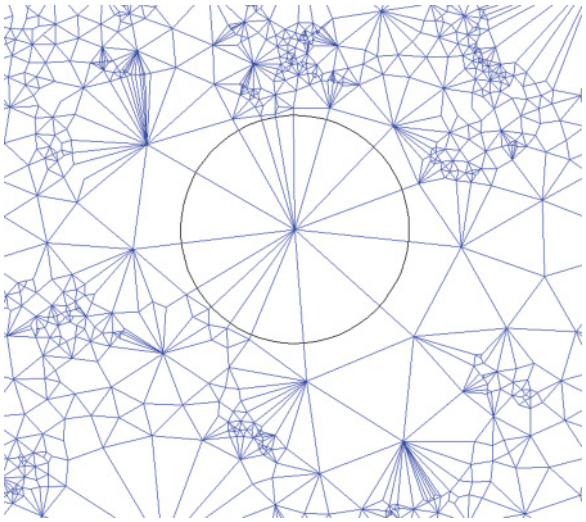

FIG. 4. (Color online) The local contact network around a typical large particle (network hub) at the ultimate state. Only the outline of the large particle is drawn for clarity. One can see the high number of contacts (degree) associated with the large particle as well as the congestion of triangles or 3-cycle topologies in the local subgraph neighborhood.

Does the ultimate state of the crushable DEM, shown to be scale free, possess small world properties? A small world network is a growing network where the typical distance between two randomly chosen nodes grows proportionally with the logarithm of the number of nodes in the network and also exhibits a high level of transitivity (i.e., nodes connected to neighbors are also connected to each other [15,16]). This means that the average path length between any two grains is small and the average clustering coefficient (i.e., the ratio of the number of 3-cycles per particle to the maximum number of 3-cycles it could be part of given the particle's degree) is large. The initial state of the DEM simulation consists of 213 particles and 334 contacts (i.e., the contact network has 213 nodes and 334 links). The limiting and ultimate state of this comminution process gives rise to a scale-free complex network of 11 877 nodes and 29 725 contact links.

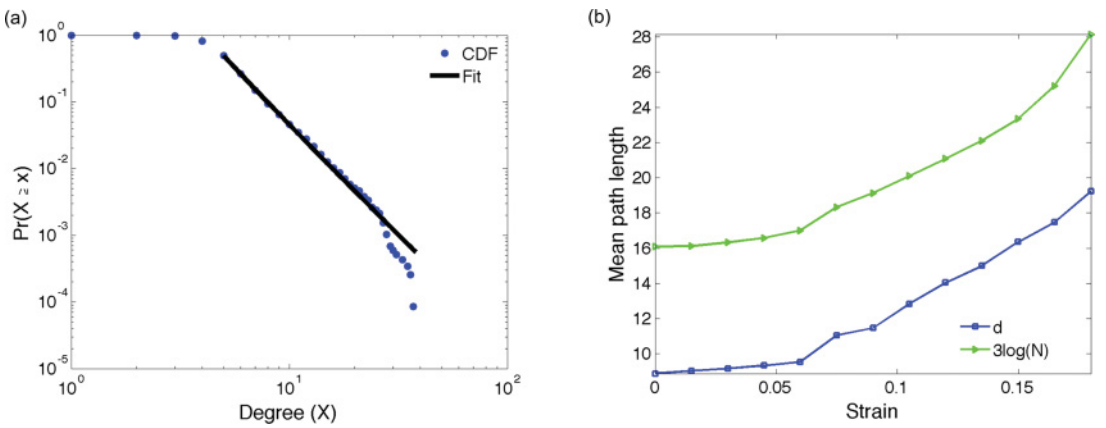

FIG. 3. (Color online) (a) Cumulative degree distribution function (CDF) of the contact network at the ultimate strain with the power law fit. (b) The scaling of the average shortest-path length d with network size is proportional to the natural logarithm $\log(N)$. Constant of proportionality of 3 is shown for illustration.

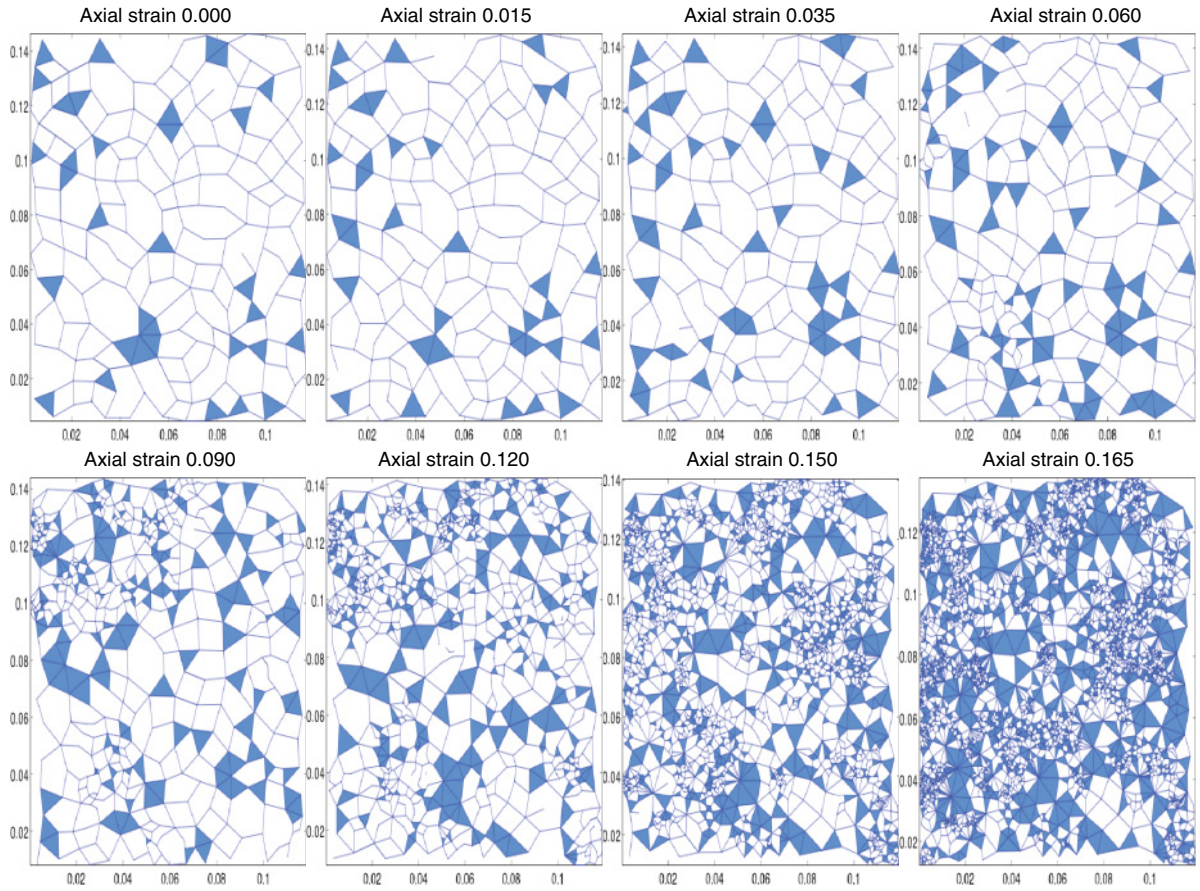

FIG. 5. (Color online) Consecutive axial strain stages of the DEM simulation (as in Fig. 1) to illustrate the development and congestion of the contact network 3-cycle population (filled triangles) as particles fracture.

The average shortest-path length between all pairs of nodes in the limiting network is 19.221 which is proportional to log(11 000) and, as expected for a growing small world network, this scaling holds for earlier axial strain states [16]. To illustrate the scaling of average shortest-path length with system size we show in Fig. 3(b) the average path length at each measured axial strain state bounded above by a constant (value of 3) times the logarithm of the number of nodes or particles in the assembly. Moreover, the average clustering coefficient for the final state network has a value of 0.3721 which is much higher than 0.0004 for an equivalent random network [16]. The presence of hubs in the ultimate state is responsible for these network features. Recall that the ultimate comminution state has large particles, which survive the comminution process, and these form hubs; see Fig. 4. In turn these hubs then introduce a conduit through which shortest paths between two particles pass. A dual mechanism is responsible for the high clustering that develops toward the ultimate state. First it is promoted by the breakage criterion which presents at least one 3-cycle initially for every grain that breaks. Second, the decreasing porosity of the sample favors locally densely packed grains in 3-cycle formations (i.e., 3 particles in mutual contact). Figure 5 shows how the contact network evolves and its 3-cycle populations congest as particles fracture and loading increases for the axial strain states shown in Fig. 1.

While small world and scale-free networks are common to the DEM model and Apollonian networks, a major difference between Apollonian networks and the contact networks of the crushable DEM model lies in the mechanism that governs the growth and evolution of the network. In the latter, new nodes and links are not added to the network in the self-similar or iterative fashion that Apollonian networks are constructed. Instead the network evolution in the crushable DEM arises from the coupled dynamics of grain breakage and grain rearrangements. The former is governed by the local breakage criterion, while the latter is determined by the physical contact law. As loading proceeds, new contacts are formed and old contacts are broken within a growing network. Hence, compared with the clean statistics of the Apollonian network construction, a richer dynamics emerges from the rheology of confined comminution that is due to the coupling between intergrain contact and grain breakage rules.

IV. INFORMATION FLOW AND SHORTEST PATHS

At this point it is worth venturing outside the confines of granular physics to explore a feature of the contact networks from our confined comminution process, which may have wider application and interest to practical manmade networks. The concept of vulnerability of a network bears an interesting interpretation with respect to the resilience and fragility of

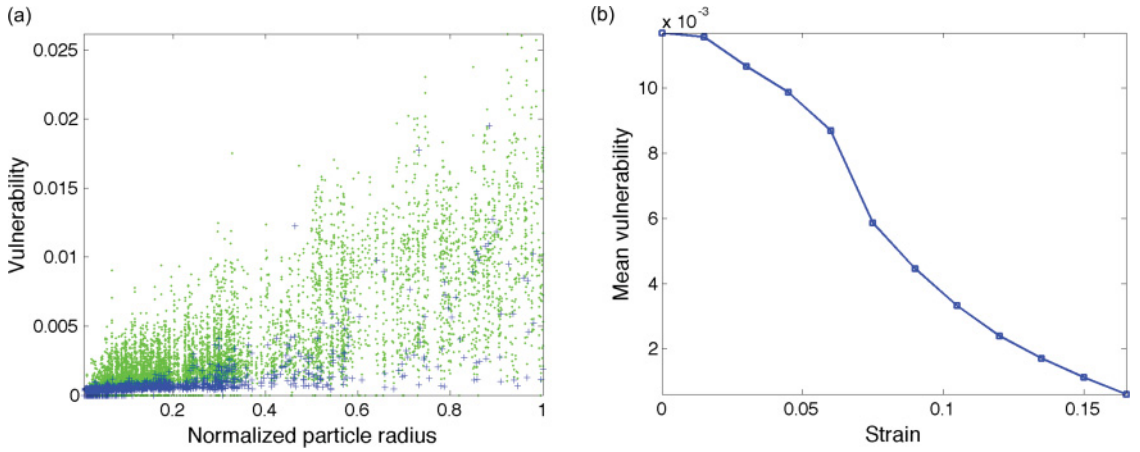

FIG. 6. (Color online) (a) Vulnerability of each node with respect to that node's normalized particle radius at each strain (green, light gray). The final strain state shown is more darkly colored blue crosses. (b) Evolution of the network mean node vulnerability toward the ultimate state.

a network. Vulnerability can help to locate the nodes of a network which are critical to its optimum performance or function. The vulnerability is based on the global efficiency E of a network, which is calculated as the average of the reciprocals of the shortest-path lengths [17]. The vulnerability of a node is found by removing it and all of its connecting links from the network. An updated efficiency E_i is calculated for this node-reduced network. The vulnerability of the removed node is $V_i = (E - E_i)/E$ [17]. For a scale-free network, it is intuitive that nodes with the highest vulnerability will be the hubs because removing these removes the most links from the network and disrupts the shortest-path routes. In the context of a complex network induced by the comminution process, it is reasonable to expect that these hubs, being the largest particles, should also be the most vulnerable. This is indeed the case exemplified in Fig. 6(a), where the nodes with the highest vulnerability are generally the largest particles. We emphasize here that node vulnerability is a network property—and not a mechanical grain property. As such, a node that is more vulnerable in the contact network does not mean the corresponding particle in the physical model is more vulnerable to fracture.

An interesting observation of wider import is that, as the fracture process proceeds to its ultimate distribution, the average vulnerability of the entire network decreases [see Fig. 6(b)]. That is, despite some nodes becoming network hubs as loading increases, the network is becoming less vulnerable. Furthermore, Fig. 6(a) shows that the hubs themselves become less vulnerable. As such, the process of comminution is developing a network with a lot of redundancy in terms of shortest paths. Sensor networks and smart grids generally require network topologies which are anisotropic and invulnerable to isolated failures and random attacks. This suggests that a sensor network design inspired by the physical comminution process creates a more resilient network since the vulnerability to losing a sensor is mitigated by the architecture.

V. SELF-ORGANIZATION OF FORCE CHAINS

We now return to a more focused granular interpretation of the evolution of contacts (or fabric) and its influence on the evolution of forces in the comminution system. In a granular material, the structures that are most important to function are those which support load (i.e., those which enable the most efficient force and energy transmission in the system). The major load-bearing structures within a granular material are the force chains, forming the primary building blocks of self-organization in dense granular materials [23–25,27]. In the network induced through the DEM comminution process, we can use force, energy, and contact information to find where the force chains are within our network [2]. Furthermore, we can, in a manner similar to Ref. [19], test whether the arrangement of these strong links (contacts) is special with respect to a null random model.

We first consider the efficiency of the comminution network in terms of weighted shortest paths. The shortest paths are determined by favoring strong contact links weighted by the (inverse) magnitude of the normal contact force. That is, the shortest-path lengths are now the sum of the reciprocal of the contact link weights and not (necessarily) the number of links traversed in each path. The efficiency is now weighted being the average of these new shortest-path lengths. We then consider an ensemble of null (random) networks [12,19,44,45], each of which is generated by reshuffling the normal contact forces while keeping all else identical to the DEM model of confined comminution. Note that these null (random) networks are statistical constructs and are not designed to serve as alternative mechanistic models to the DEM. By solely randomizing the allocation of normal contact forces in the contact links, we preserve the topological connectivity of the DEM model of confined comminution. The (weighted) efficiency of the resulting random force network is calculated, and a distribution of the efficiencies for all the network realizations in the ensemble is generated. We then ask: where in this distribution does the efficiency of the original contact force network lie? Does the confined comminution process lead to a relatively efficient transmission of force?

In Figs. 7(a) and 7(b), we show the original force network for a representative strain and one of the randomized surrogate networks. In Fig. 7(c), we also see evidence for self-organization throughout the loading: for all strains, the efficiency of the original network is well into the tails of the surrogate distributions and, furthermore, it is always a higher

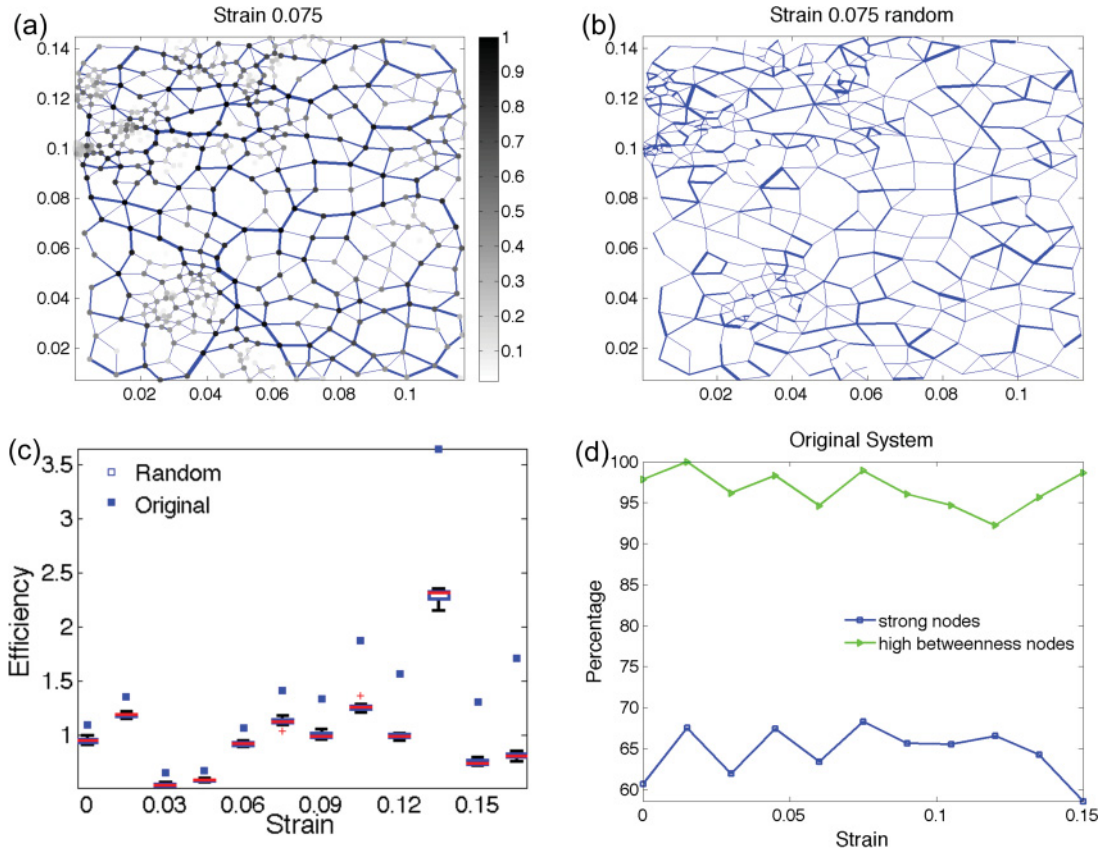

FIG. 7. (Color online) (a) Contact network for a representative strain with strength of normal contact force indicated by line thickness. Nodes are ranked by their betweenness (gray scale light to dark show low to high values). (b) Randomized network preserving connectivity. (c) Efficiency distribution of the randomized networks and the original network throughout loading. (d) Percentages of above average betweenness nodes that form strong contacts (green, light gray), and strong contact nodes that have above average betweenness throughout loading (blue, dark gray) for the original system.

value. That is, the material is rearranging and distributing the load in a manner more systematic than a random distribution. It should be noted that the randomized networks only preserve the contact topology and they are unlikely to satisfy force balance equations nor be mechanically meaningful as mentioned earlier. That said, other randomization tests which vary the contact topology are also possible which preserve particular aspects of the real network under consideration; for example, the degree of a node (coordination number) or the number of minimal cycles of a particular length [46]. It is reassuring that the weighted efficiency measure can distinguish between a self-organized force network and a randomized one. In randomization tests and hypothesis testing in general [47,48], a next step when simple random models can be rejected is to introduce more complicating aspects of the network under consideration (e.g., realistic rules regarding force transmission). One such progression would be randomizing the forces subject to the constraint of force balance, if indeed this is possible. This is the subject of ongoing research.

We are also able to shed light on the possible choices the material is selecting to produce such a self-organized strong force network. The strong contact network is the subnetwork of contacts that bears the majority (above average normal force) of the load. A common protocol in communication is to send data packets through a network using optimized shortest-path routing. Solely from the topology of the network we can gauge which links, or nodes, bear the heaviest traffic using the concept of betweenness (nodes are ranked by the number of shortest paths they are a part of) [49]. Figure 7(a) shows the strong contacts join high-betweenness nodes. If we now consider the nodes within the original strong contact network and compare them to the nodes having greater than average betweenness, then we find that more than 60% of strong contact nodes have above average betweenness throughout loading. Moreover, greater than 90% of nodes with above average betweenness are associated with strong contact links [see Fig. 7(d)]. This provides evidence that the rheological response of the granular material is to rearrange itself so that the load can be distributed throughout the assembly in an efficient manner similar to a shortest-path data-routing protocol.

An equally important aspect of granular comminution rheology uncovered here is that topology bears a major but not exclusive governing influence on the process of force transmission. That around 40% of the strong contacts connect particles with high-low and low-low betweenness suggest another factor is at play. In the context of force transmission formulated as an optimization problem, we envisage that multiple constraints are needed to properly capture the various factors that drive self-organization of forces in comminution systems.

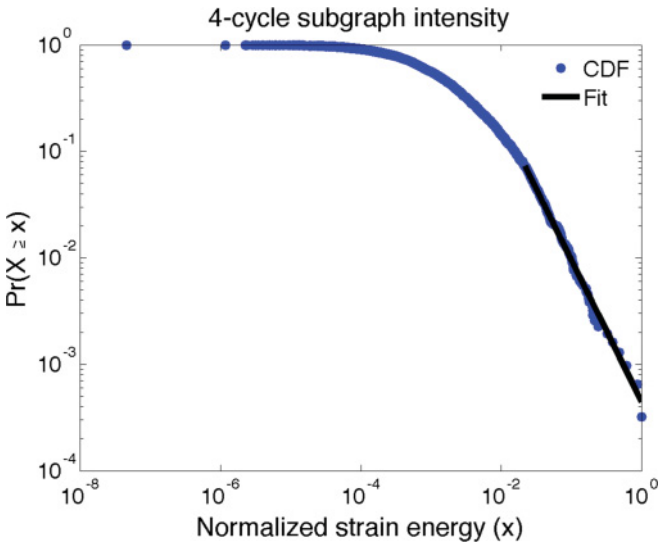

FIG. 8. (Color online) Cumulative distribution and power law fit for the 4-cycle intensities based on normalized strain energy at contacts.

VI. ENERGY INTENSITIES OF 3- AND 4-CYCLE MOTIFS

From previous studies on the self-organization of force chains and their lateral support, we found that the strongest surviving force chains are conjoined with 3-cycle network motifs (triangles) [23]. We can weight the contacts in cycle motifs by a meaningful quantity such as the contact strain energy—an extension of the previous weighting by others (e.g., normal contact force by including shear contact forces and material properties as was done in [50] and the work networks of [10]). Calculations of the subgraph intensity of the various n-cycles ($n \geqslant 3$), which represents the geometric mean of the subgraph contact link weights, can reveal how strong each cycle motif is [51]. A power law fit to the distribution of 3-cycle subgraph intensities fails to pass a KS test for significance. From a rheological perspective, this means that, despite 3-cycle motifs being superb and important stabilizing agents for force chains, owing to their ability to frustrate relative rotations and thereby resist force chain buckling, there is only so much energy they can store within their structure before they break contacts and release energy. By contrast, the 4-cycle (squares) normalized subgraph intensity distribution is consistent with a continuous power law distribution $p(x) = \frac{\alpha-1}{x_{\min}}(\frac{x}{x_{\min}})^{-\alpha}$ with $\alpha = 2.3319$ for $x_{\min} = 0.0219$ (see Fig. 8). The value obtained from the fit of α means that the distribution of 4-cycle intensities using strain energy as the link weight has a finite mean but infinite variance. Thus, there is a small nonzero probability that 4-cycles can store large amounts of energy at their contacts. A possible explanation for this is that the topology of 4-cycles allow relative rotations and so they can store more energy because they can rearrange more easily without breaking contact and release of energy. Such structures, therefore, can act as "lubricants" because of their roller-bearing-like quality (cf. space-filling bearings [52] and bichromatic packings of Ref. [53], which are rich in 4-cycles).

VII. CONCLUSION

In summary, we have examined the process of comminution within the framework of complex networks with the intent of relating the dynamics that occurs on such networks to rheological behavior. We have shown that the contact networks evolve to a network possessing a degree distribution consistent with a power law. The networks also exhibit small world properties and 3-cycle topologies are anisotropically and densely distributed throughout the material. Furthermore, by examining node betweenness and strong contact link correlations, we found that force transmission appears to be following a shortest-path data-routing communication protocol. Contact topology has a significant but not exclusive influence on the self-organization of force chains. In examining the energy intensity of 3- and 4-cycle motifs in the ultimate state, we discovered that the distribution of subgraph intensity for 4-cycle contacts was consistent with a power law with a parameter less than three. This suggests that 4-cycle topologies are capable of storing vast amounts of energy within their contacts. The role of 4-cycles in energy transmission thus warrants further study and is the subject of ongoing work.

ACKNOWLEDGMENTS

We thank Oded Ben-nun for data availability and funding by the ARC (DP0986876), the US ARO (W911NF-07-1-0370 & W911NF-11-1-0175), and the Melbourne Energy Institute. MS thanks Hong Kong Polytechnic University Grant No. G-U67 for support.

[1] O. Ben-Nun and I. Einav, Philos. Trans. R. Soc. London A **368**, 231 (2010).
[2] O. Ben-Nun, I. Einav, and A. Tordesillas, Phys. Rev. Lett. **104**, 108001 (2010).
[3] Y. P. Cheng, M. D. Bolton, and Y. Nakata, Geotechnique **54**, 131 (2004).
[4] C. G. Sammis, G. King, and R. Biegel, Pure Appl. Geophys. **125**, 777 (1987).
[5] M. R. Coop, K. K. Sorensen, T. Bodas, and G. Georgoutsos, Geotechnique **54**, 157 (2004).
[6] D. L. Turcotte, J. Geophys. Res. **91**, 1921 (1986).
[7] J. A. Yamamuro, P. A. Bopp, and P. V. Lade, J. Geotech. Eng. **122**, 147 (1996); Y. Nakata, Y. Kato, M. Hyodo, A. F. L. Hyde, and H. Murata, Soils Found., J. Japn. Geotechnical Soc. **41**, 39 (2001); G. R. McDowell and C. M. Daniell, Geotechnique **51**, 173 (2001).
[8] J. A. Dodds and P. J. Lloyd, Powder Technol. **5**, 69 (1972).
[9] T. Aste, Phys. Rev. E **53**, 2571 (1996).
[10] N. P. Kruyt and S. J. Antony, Phys. Rev. E **75**, 051308 (2007).

[11] L. Rothenburg and N. P. Kruyt, Int. J. Solids Struct. **41**, 5763 (2004).
[12] M. E. J. Newman, *Networks: An Introduction* (Oxford University Press, Great Clarendon Street, Oxford, 2010).
[13] E. Estrada, Lect. Notes Comput. Sci. **6218**, 45 (2010).
[14] M. E. J. Newman, SIAM Rev. **45**, 167 (2003).
[15] D. J. Watts and S. H. Strogatz, Nature (London) **393**, 440 (1998).
[16] R. Albert and A.-L. Barabási, Rev. Mod. Phys. **74**, 47 (2002).
[17] F. Costa, F. A. Rodrigues, G. Travieso, and P. R. Villas, Adv. Phys. **56**, 167 (2007).
[18] S. Boccaletti, V. Latora, Y. Moreno, M. Chavez, and D.-U. Hwang, Phys. Rep. **424**, 175 (2006).
[19] A. Smart and J. M. Ottino, Soft Matter **4**, 2125 (2008).
[20] D. M. Walker and A. Tordesillas, Int. J. Solids Struct. **47**, 624 (2010).
[21] P. G. Lind, M. C. González, and H. J. Herrmann, Phys. Rev. E **72**, 056127 (2005).
[22] D. M. Walker, A. Tordesillas, C. Thornton, R. P. Behringer, J. Zhang, and J. F. Peters, Granular Matter **13**, 233 (2011).
[23] A. Tordesillas, D. M. Walker, and Q. Lin, Phys. Rev. E **81**, 011302 (2010).
[24] A. Tordesillas, S. Pucilowski, D. M. Walker, J. F. Peters, and M. Hopkins, Dynamics of Continuous, Discrete and Impulsive Systems B (2011) (to be published).
[25] R. Arévalo, I. Zuriguel, and D. Maza, Phys. Rev. E **81**, 041302 (2010).
[26] A. Tordesillas, P. O'Sullivan, D. M. Walker, and Paramitha, Comptes Rendus Mecanique **338**, 556 (2010).
[27] A. Tordesillas, Q. Lin, J. Zhang, R. P. Behringer, and J. Shi, J. Mech. Phys. Solids **59**, 265 (2011).
[28] O. Tsoungui, D. Vallet, and J. C. Charmet, Powder Technol. **105**, 190 (1999).
[29] M. Muthuswamy and A. Tordesillas, J. Stat. Mech. (2006) P09003.
[30] J. C. Jaeger, J. Rock. Mech. **4**, 219 (1966).
[31] W. Weibull, J. Appl. Mech. (Trans. ASME) **18**, 293 (1951).
[32] J. A. Astrom and H. J. Herrmann, Eur. Phys. J. B **5**, 551 (1998).
[33] S. S. Manna and H. J. Herrmann, J. Phys. A **24**, L481 (1991).
[34] P. S. Dodds and J. S. Weitz, Phys. Rev. E **67**, 016117 (2003).
[35] G. W. Delaney, S. Hutzler, and T. Aste, Phys. Rev. Lett. **101**, 120602 (2008).
[36] A. J. Liu and S. R. Nagel, Nature (London) **396**, 21 (1998); E. Aharonov and D. Sparks, Phys. Rev. E **60**, 6890 (1999); H. A. Makse, D. L. Johnson, and L. M. Schwartz, Phys. Rev. Lett. **84**, 4160 (2000).
[37] R. Biegel, C. G. Sammis, and J. H. Dieterich, J. Struct. Geol. **11**, 827 (1989).
[38] I. Einav, J. Mech. Phys. Solids **55**, 1274 (2007).
[39] R. Pastor-Satorras and A. Vespignani, Phys. Rev. Lett. **86**, 3200 (2001).
[40] J. S. Andrade, H. J. Herrmann, R. F. S. Andrade, and L. R. da Silva, Phys. Rev. Lett. **94**, 018702 (2005).
[41] M. Small, D. M. Walker, and C. K. Tse, Phys. Rev. Lett. **99**, 188702 (2007).
[42] M. Small, X. Xu, J. Zhou, J. Zhang, J. Sun, and J. Lu, Phys. Rev. E **77**, 066112 (2008).
[43] A. Clauset, C. R. Shalizi, and M. E. J. Newman, SIAM Rev. **51**, 661 (2009); Companion toolbox [http://www.santafe.edu/aaronc/powerlaws/].
[44] R. Milo, S. Shen-Orr, S. Itzkovitz, N. Kashtan, D. Chklovskii, and U. Alon, Science **298**, 824 (2002).
[45] M. E. J. Newman, S. H. Strogatz, and D. J. Watts, Phys. Rev. E **64**, 026118 (2001).
[46] S. Maslov, K. Sneppen, and A. Zaliznyak, Physica A **333**, 529 (2004).
[47] T. Schrieber and A. Schmitz, Physica D **142**, 346 (2000).
[48] M. Small and C. K. Tse, IEEE Trans. Circuits Syst. I **50**, 663 (2003).
[49] M. E. J. Newman, Social Networks **27**, 39 (2005).
[50] A. Tordesillas, Philos. Mag. **87**, 4987 (2007).
[51] J-P. Onnela, J. Saramäki, J. Kertész, and K. Kaski, Phys. Rev. E **71**, 065103 (2005).
[52] H. J. Herrmann, G. Mantica, and D. Bessis, Phys. Rev. Lett. **65**, 3223 (1990).
[53] H. J. Herrmann, J. A. Astrom, and R. Mahmoodi Baram, Physica A **344**, 516 (2004).